AIP | The Journal of Chemical Physics

First principle structural determination of (B2O3)n (n = 1–6) clusters: From planar to cage

Lifen Li and Longjiu Cheng

Citation: J. Chem. Phys. **138**, 094312 (2013); doi: 10.1063/1.4793707
View online: http://dx.doi.org/10.1063/1.4793707
View Table of Contents: http://jcp.aip.org/resource/1/JCPSA6/v138/i9
Published by the American Institute of Physics.

First principle structural determination of $(B_2O_3)_n$ (n = 1–6) clusters: From planar to cage

Lifen Li (李丽芬) and Longjiu Cheng (程龙玖)[a)]
School of Chemistry and Chemical Engineering, Anhui University, Hefei, Anhui 230039, People's Republic of China

(Received 18 November 2012; accepted 14 February 2013; published online 5 March 2013)

The structure of $(B_2O_3)_n$ clusters (n = 1–6) are investigated using the method combining the genetic algorithm with density functional theory. Benchmark calculations indicate that TPSSh functional is reliable in predicting the energetic sequences of different isomers of $(B_2O_3)_n$ cluster compared to the high-level coupled cluster method. The global minimum (GM) structures of $(B_2O_3)_n$ clusters are planar up to n = 3, and cages at n = 4–6. A T_d fullerene is found in the GM structure at n = 6. The stability of three-dimensional structures increases with the size of the cluster according to the analysis of the calculated atomization energy. Natural bonding analysis given by adaptive natural density partitioning reveals delocalized π-bonding in the 4-membered and 6-membered rings, and it is aromatic at the centers of cages and rings. © *2013 American Institute of Physics*. [http://dx.doi.org/10.1063/1.4793707]

I. INTRODUCTION

Much attention has been attracted by boron and boron-based clusters because of their interesting physical and chemical properties. Boron is an element capable of forming strong covalent bonds and possesses an astounding variety of chemistry. Experimental and theoretical studies on the electronic structure,[1–4] chemical bonding,[5–7] and spectroscopic properties[8–15] of bare boron clusters as well as doped boron clusters[16–19] have been reported. By replacing pairs of neighboring C atoms with alternating B and N atoms, one can produce graphite-like boron nitride sheets and nanotubes, quite analogous to nanotubes of carbon. A number of studies on the molecular, electronic structures, the spectroscopic, and the thermo-chemical properties of small boron oxide clusters have been reported. Anderson and co-workers[20–25] experimentally investigated the oxidation of boron clusters and the subsequent reactions of the $B_nO_m^+$ cations with small molecules in the gas phase. Wang and co-workers[14,26] used experimental photoelectron spectroscopy coupled with quantum chemical calculations to probe the electronic structures of small anions including $B_3O_2^-$, $B_4O_2^-$, $B_4O_3^-$, $B_4O_2^{2-}$ and their neutral counterparts. Most of the theoretical studies have focused on B_nO_m species whose relationship of n and m leaves stoichiometry,[27–43] and diboron trioxide $(B_2O_3)_n$ clusters received little attention. Diboron trioxide is not only an important material in the ceramic and glass technology,[44] but also an interesting material from a solid-state-physical point of view due to its optical characteristics.[45] At normal pressure, B_2O_3 has a trigonal structure (B_2O_3-I) characterized by a three-dimensional network of corner-linked BO_3 triangles.[46,47] At high pressure, an orthorhombic modification (B_2O_3-Π) is more stable. It consists of a framework of linked BO_4 tetrahedra.[48]

Many achievements have been made in the modeling of oxides (e.g., Al_2O_3 and Fe_2O_3).[49–52] Recently, Woodley[53] reported the stable and metastable stoichiometric $(X_2O_3)_n$ clusters of boron, aluminum, gallium, indium, and thallium oxide defined using classical interatomic potentials. The method is effective to the ionic compound as Woodley reported. However, the structure of boron oxide, as far as we know, is not supposed similar with that of alumina since boron atom prefers to form covalent bond with oxygen atom.

Therefore, we adopted density functional theory (DFT) method combined with genetic algorithm (GA) to predict the structure of $(B_2O_3)_n$ (n = 1–6) clusters. The results show that the global minimum structures of $(B_2O_3)_n$ vary with n from plane (n = 1–3) to cage (n >3), which are indeed different from those of $(Al_2O_3)_n$. And a T_d fullerene is found to be the global minimum of $(B_2O_3)_6$.

II. COMPUTATIONAL DETAILS

A. Global optimization method

The low-energy isomers of $(B_2O_3)_n$ clusters were located by the combination of GA and DFT method, which has been successfully applied in the structural prediction of a number of systems.[50,54–59] All DFT calculations were accomplished by the GAUSSIAN 09 package[60] using the TPSSh functional.[61] In global research of the potential energy surface, a small basis set (3-21G) is used for saving time. After global optimization, the low-lying TPSSh/3-21G isomers are fully relaxed at TPSSh/6-311+G* level of theory.

B. Benchmark calculations

For boron clusters, different functionals of DFT methods make great difference in predicting the energetic sequences of different isomers.[56,62] To verify the reliability of different functionals in the prediction of $(B_2O_3)_n$ clusters, a

[a)]Author to whom correspondence should be addressed. Electronic mail: clj@ustc.edu. Tel./Fax: +86-551-5107342.

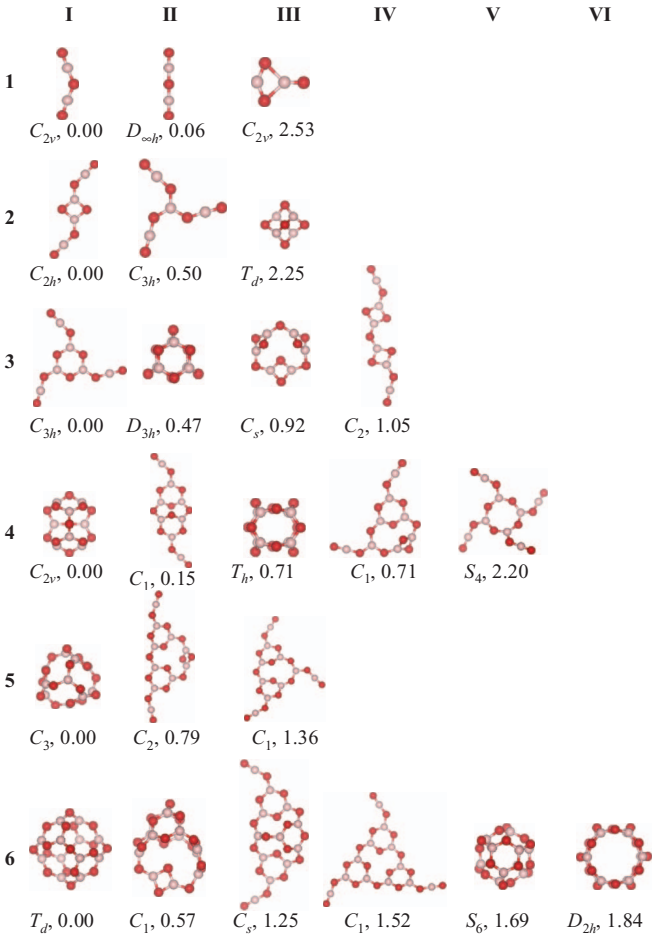

FIG. 1. The low-energy isomers of $(B_2O_3)_n$ (n = 1–6) clusters. The structures in column **I** correspond to the global minima; columns **II**–**VI** correspond to isomers that are higher in energy, and the symmetry and the relative energies in eV are labeled. O-red; B-pink.

benchmark calculation is carried out by comparing the relative stability of the three isomers of $(B_2O_3)_2$ (see structures in Figure 1) in different methods. Results of the benchmark calculation are given in Table I to compare different functionals (TPSSh, PBE0,[63] M06,[64] B3LYP,[65] and BPW91[66,67]) with the high-level coupled cluster method (CCSD(T)/aug-cc-pvtz).[68] Note that TPSSh and PBE0 functionals are consistent with CCSD(T) method in relative stability of the three isomers. However, relative stability of the planar isomers (2**II** and 2**III**) is highly overestimated by M06, B3LYP, BPW91, and BP86 functionals (especially for B3LYP functional, where the relative energy of the planar isomer (2**I**) is undervalued by even 0.69 eV (2.94–2.25) compared to the 3D isomer (2**III**)). TPSSh/6-311+G* method is in reasonable agreement with CCSD(T)/aug-cc-pvtz method tending to underestimate the planar structure 2**II** about 0.05 eV, which suggests that TPSSh/6-311+G* method is reliable in predicting relative stability of different packings of $(B_2O_3)_n$ clusters.

TABLE I. Comparison of single point energies for the three low-lying isomers of $(B_2O_3)_2$ (see structures in Figure 1).[a]

Method	2**I**	2**II**	2**III**
CCSD(T)[b]	− 550.4027577	0.55	2.25
TPSSh	− 551.326837	0.50	2.25
PBE0	− 550.713299	0.57	2.16
M06	− 551.090825	0.41	2.41
B3LYP	− 551.344355	0.30	2.94
BPW91	− 551.261793	0.41	2.61

[a]Energies for 2**I** are in atomic units, other energies are relative to this in eV. Results are single point energies with 6-311+G* basis sets for TPSSh/6-311+G* geometry.
[b]The basis set is aug-cc-pvtz for CCSD(T).

III. RESULTS AND DISCUSSION

Combing the GA with DFT method, we obtained the low-energy isomers for $(B_2O_3)_n$ (n = 1–6) clusters at the TPSSh/6-311+G* level. Figure 1 plots the low-energy isomers of $(B_2O_3)_n$ (n = 1–6) clusters. All the isomers are verified to be true local minima by frequency check (except for the 1**II**, which is a saddle point on the energy landscape). The global minima (GMs) are planar (up to $n = 3$), and cage at n = 4–6, and the energy gap between the lowest-energy planar and cage isomers is relatively large except for $n = 4$. The electronic state, symmetry, energy gap, and atomization energy of structures for each isomers of $(B_2O_3)_n$ (n = 1–6) clusters are listed in Table II.

TABLE II. Electronic state[a], symmetry[b], energy gap[c], atomization energy[d] and NICS value[e] of structures for $(B_2O_3)_n$ (n = 1–6) clusters.

N	ES[a]	Symmetry[b]	Δ_{HL}[c]	E_{at}[d]	NICS[e]
1**I**	$^1A_1$	C_{2v}	7.56	27.46	
1**II**	$^1\Sigma_g$	D_h	7.58	27.40	
2**I**	^1A_g	C_{2h}	7.74	28.81	−9.26
2**II**	$^1A'$	C_{3h}	7.55	28.56	
2**III**	$^1A_1$	T_d	3.86	27.68	−9.80
3**I**	$^1A'$	C_{3h}	7.44	29.58	−4.54
3**II**	$^1A_1{}'$	D_{3h}	5.71	29.43	−8.10
3**III**	$^1A'$	C_s	7.09	29.28	−4.73
3**IV**	^1A	C_2	7.67	29.23	
4**I**	$^1A_1$	C_{2v}	6.84	30.07	−6.46
4**II**	^1A_g	C_1	6.79	30.03	−5.68
4**III**	^1A_g	T_h	5.58	29.89	−5.77
4**IV**	^1A	C_1	7.17	29.89	
4**V**	^1A	S_4	6.49	29.52	−0.47
5**I**	^1A	C_3	7.19	30.48	−5.14
5**II**	^1A	C_2	7.46	30.32	−2.10
5**III**	^1A	C_1	7.09	30.20	−3.08
6**I**	$^1A_1$	T_d	7.30	30.76	−2.34
6**II**	^1A	C_1	7.63	30.66	−1.92
6**III**	$^1A'$	C_s	7.47	30.55	−0.95
6**IV**	^1A	C_1	7.35	30.50	−0.16
6**V**	^1A_g	S_6	6.95	30.48	−1.60
6**VI**	^1A_g	D_{2h}	5.77	30.45	−1.72

[a]Electronic state.
[b]Point group (symmetry).
[c]Energy gaps (eV) between the highest occupied molecular orbital and lowest unoccupied molecular orbital.
[d]Average atomization energy, where $E_{at} = [E(B_2O_3)_n - 2n*E(B) - 3n*E(O)]/n$.
[e]Nucleus independent chemical shift values (ppm) in cluster centers at the TPSSh/6-311+G* level.

A. Geometry structures

$(B_2O_3)_1$: the GM of $(B_2O_3)_1$ (1**I**) is a V-shaped configuration with the B-O bond-distances of 1.21 Å and 1.33 Å and the B-O-B bond angle of 139.3°. Linear structure 1**II** is a saddle point, which is only 0.06 eV higher in energy than 1**I**. 1**III** is the most stable structure of $(Al_2O_3)_1$, which is 2.53 eV higher in energy than 1**I**.[69]

$(B_2O_3)_2$: 2**I** is planar with a 4-membered ring (BOBO) and two tails (-OBO) attached to the two B atoms of the rhombus. As well as a planar structure, 2**II** is constituted of a BO_3 triangle and three boronyls (-BO). 2**III** in T_d symmetry is the most stable configuration of $(Al_2O_3)_2$, which is 2.25 eV higher in energy.[50,52,69]

$(B_2O_3)_3$: In the lowest energy configuration of $(B_2O_3)_3$ (3**I**), there are three tails (-OBO) attached to the planar hexagonal B_3O_3 unit. 3**II** is 0.47 eV higher in energy than 3**I**, which is the most stable cage structure of $(Al_2O_3)_3$.[50,52,69] 3**III** lies 0.92 eV higher in energy whereas 3**IV** lies 1.05 eV higher in energy.

$(B_2O_3)_4$: The GM (4**I**) is a cage configuration in C_{2v} symmetry, and stacks of two 6-membered (chairlike) rings and two 8-menbered rings. 4**I** is consistent with the result of Woodley.[53] The second low-lying isomer (4**II**) is quasi-planar with two 6-membered rings and an 8-membered ring. 4**II** is 0.15 eV higher in energy at TPSSh/6-311+G* while is even more stable at B3LYP/6-311+G* by 0.22 eV. 4**III**(T_h) is 0.71 eV higher in energy. 4**IV** has a 4-membered ring, a 6-membered ring and a trigonal BO_3 unit, which is the lowest-energy cage isomer of $(Al_2O_3)_4$.[50,52,69] 4**V** is quasi-planar with an 8-membered ring and 4 tails (-OBO) and is 2.20 eV higher in energy.

$(B_2O_3)_5$: The most stable structure of $(B_2O_3)_5$ (5**I**) is a chiral C_3 cap. The quasi-planar structure 5**II** (C_2) consists of two 6-membered rings and one 4-membered ring and is 0.79 eV higher in energy than 5**I**. 5**III** (C_1) consists of two 6-membered rings and one trigonal BO_3 unit.

$(B_2O_3)_6$: A fullerene cage 6**I** with tetrahedral symmetry is suggested as the most stable structure of $(B_2O_3)_6$. It can be regarded as four 6-membered rings occupying the four vertexes and another six B atoms capping the edges of the tetrahedron, which consists of four 6-membered rings and four 12-membered rings. 6**II** is a 3D structure with three chairlike hexagonal B_3O_3 units and a B_2O_2 planar rhombus. 6**III** is quasi-planar with three 6-membered rings and a trigonal BO_3 unit. It is 1.25 eV higher in energy. 6**IV** (C_1) is a quasi-planar structure with three 6-membered rings. A S_6 isomer (6**V**) is found with 1.69 eV higher in energy. 6**VI** is a D_{2h} cage with 1.84 eV higher in energy.

B. Atomization energy

The calculated atomization energy (average interaction energy per B_2O_3 formula unit in the cluster: $E_{at} = [E(B_2O_3)_n - 2n*E(B) - 3n*E(O)]/n$) versus cluster sizes (the number of formula units in the cluster) is plotted for the lowest-energy (quasi-)planar and cage isomers in Figure 2(a). It is clearly seen that the atomization energy increases with cluster size increasing. The atomization energy of (quasi-)planar structures is higher than that of cages at $n \leq 3$, and the cages exceed at $n \geq 4$. This conclusion is more vividly shown in Figure 2(b) which plots the relative energy between the lowest-energy structures of the two different groups.

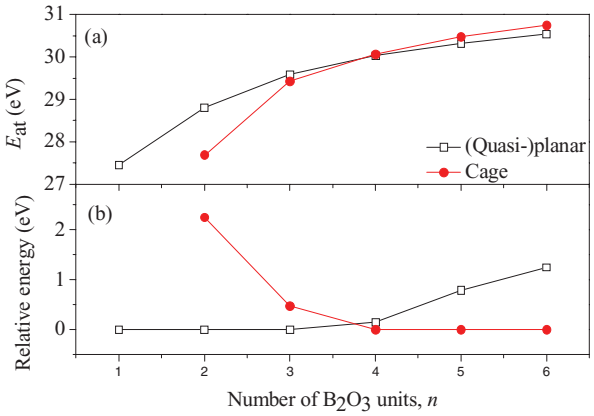

FIG. 2. (a) Atomization energy per B_2O_3 unit (E_{at}) of B_2O_3 clusters with the lowest-energy structures of different families ((quasi-)planar structures and cages) as a function of the number of B_2O_3 units n, where $E_{at} = [E(B_2O_3)_n - 2n*E(B) - 3n*E(O)]/n$; (b) Relative energies between the lowest-energy structures of different families (planar and cage structures) as a function of the number of B_2O_3 units n.

Additionally, the energy gap (E_{HL}) between the highest occupied molecular orbital (HOMO) and lowest unoccupied molecular orbital (LUMO) is an important factor influencing the structural stability. The E_{HL} of all structures are large (3.86 ∼ 7.74 eV). 2**III** have relatively small E_{HL} (3.86 eV), as a consequence of the instability of its geometry (the tension is too large because of the small bond angel).

C. Electronic structure

The low-lying isomers of $(B_2O_3)_n$ clusters are (quasi-) planar and cage, just like C_n and B_n clusters, which are resulted by delocalized electrons. Are there delocalized electrons in $(B_2O_3)_n$ clusters? Since delocalization always associated with aromaticity, we focus on the aromaticity of the $(B_2O_3)_n$ clusters first. The nucleus independent chemical shifts (NICS) value is a popular magnetic criterion of aromaticity.[70] Table II gives the NICS value at the center of some isomers for $(B_2O_3)_n$ cluster. The results show that most of isomers are aromatic, and only a few isomers are non-aromatic, but none of them is anti-aromatic. Besides, we note that all GMs of $(B_2O_3)_n$ clusters are aromatic based on NICS values listed in Table II. To the (quasi-)planar structures with one ring (2**I**, 3**I**, and 4**V**), the degree of aromaticity (NICS = −9.26, −4.54, and −0.47 ppm) reduce as the cluster size increase, as well as the prism-like structures (3**II**, 4**III**, 6**VI** corresponding to the NICS value −8.10, −5.77, −4.55, and −1.72 ppm, respectively). The reason may be that electron delocalization is harder at a larger ring. Similar to other fullerene-like structure,[71] 6**I** is aromatic too (NICS = −2.34 ppm).

According to the aromaticity of $(B_2O_3)_n$ cluster, we infer that there must be delocalized electrons among the clusters. In order to get insight into the delocalized orbital and

bonding style of $(B_2O_3)_n$ clusters, canonical molecular orbital (MO) analysis and Adaptive natural density partitioning (AdNDP) is adopted. AdNDP is a new theoretical tool developed by Zubarev and Boldyrev[72] for analysis of chemical bonding and has been successfully applied recently to the analysis of chemical bonding in clusters[71–73] and organic aromatic molecules,[73] as well as boron and gold clusters.[54,56,72,73] In the following we pick some representative structures to discuss their electronic structures.

For $n = 1$, the V-shaped structure is more stable than the linear structure. Why is the V-shaped structure more stable? Here, we first focus on the nature of the bonding of the linear structure 1**II** (Figure 3(a)). The distance between the B atom and the adjacent terminal O atom in the linear structure is 1.21 Å, and that between the B atom and the central O atom is 1.31 Å. Note that B-O single bond in the B_2O_3 crystal is 1.37 Å, the B-O double bond in BO_2 is 1.26 Å, and the B-O triple bond in BO molecule is 1.20 Å.[46,74] The chemical bonding between B atom and the terminal O atom is a triple bond, and that between B atom and the central O atom is a single bond (the Lewis structure showed in Figure 3(a)). There must be delocalized electrons in the structure. Note that 1**II** has 24 valence electrons ($3 \times 2 + 6 \times 3$), with each boron atom contributing three valence electrons and each oxygen atom contributing six valence electrons. Eight electrons are localized along the four B-O σ-bonds. The canonical π-MOs (Figure 3(a)) show that there are 12 π-electrons delocalized on the whole molecule in two vertical directions in 1**II**. All of the atoms of the linear structure are in *sp* hybridization. The remaining 4 electrons are two lone pairs (LPs) on the other *sp* hybrid orbital of the terminal oxygen. The bond lengths (1.21 Å and 1.33 Å) and the π-MOs of V-shaped structure (Figure 3(b)) are similar to the linear structure. Note that the angel of the V-shaped structure is 139.3°, which indicates that the hybridization of the central oxygen atom is between *sp* and sp^2 hybridization. In order to confirm this speculation, we applied AdNDP analysis to the two isomers. According to AdNDP analysis, there are two LPs (occupied number (ON) = 1.96 |e|, which is close to the ideal limit of 2.00|e|), four two-center two-electron (2c-2e) σ-bonds (ON = 1.99–2.00 |e|), four 2c-2e π-bonds (ON = 2.00 |e|), and two 3c-2e σ-bonds (ON = 1.96 |e|) in 1**II** (Figure 3(d)). The results show that the chemical bonding between B atom and the terminal O atom and that between B atom and the central O atom are, as the supposition to the Lewis structure, triple bonds and single bonds, respectively. 1**I** is a distortion of 1**II**, and the two have similar bonding patterns (Figure 3(c)). The two electrons in *x-y* plane of central oxygen atom of 1**I** can be considered as 3c-2e bond (ON = 1.96 |e|) or LP (ON = 1.82 |e|) which probes that the hybridization of the central O atom of the V-shaped structure is between *sp* and sp^2. The reason why the V-shaped structure is favored more may be that the oxygen atom prefers more sp^2 hybridization.

$(B_2O_3)_2$ adopts a C_{2h} ground state geometry with a 4-membered ring which is, generally speaking, unstable in covalence compounds. Why is the 4-membered ring stable in the GM of $(B_2O_3)_2$ cluster? The nature of the bonding of 2**I** is analyzed first. The B-O bond lengths in 2**I** are 1.21 Å for the distance of the terminal B-O bonds and 1.33–1.40 Å for others (Figure 4(a)). Compared with the triple bond length (1.20 Å) and the single bond length (1.35 Å), we suppose the

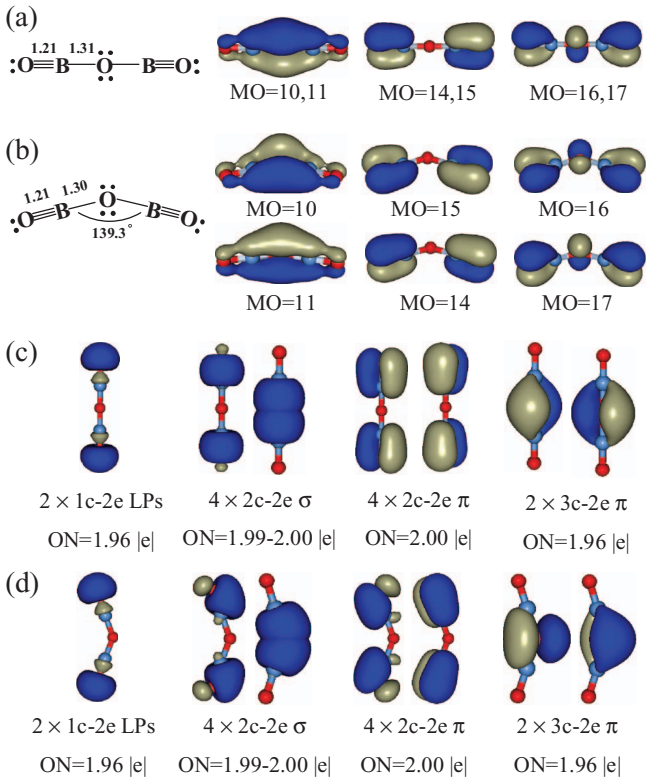

FIG. 3. (a) Lewis representation and π-MOs of 1**II**; (b) molecular structure and π-MOs of 1**I**; (c) AdNDP localized bonding patterns of structure 1**II**; (d) AdNDP localized bonding patterns of structure 1**I**. B-blue, O-red.

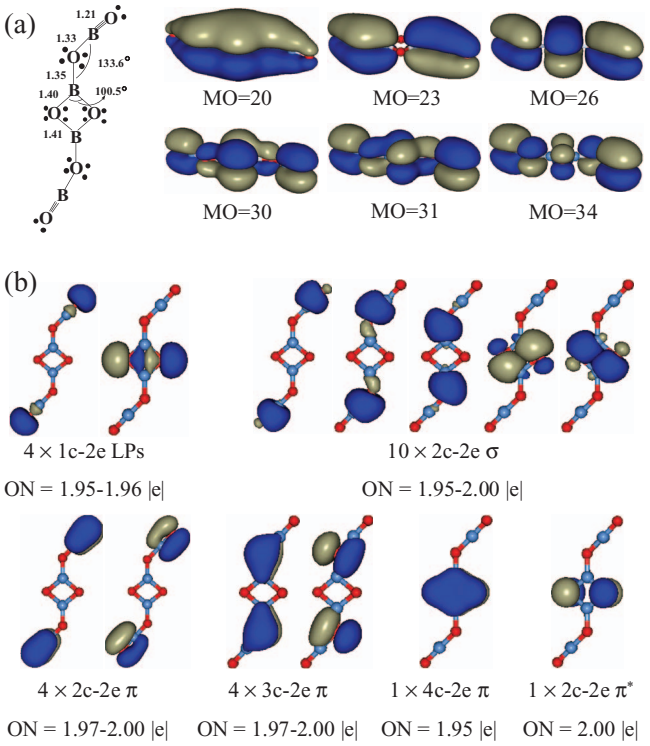

FIG. 4. (a) Lewis representation and π-MOs of 2**I**; (b) AdNDP localized bonding patterns of 2**I**. B-blue, O-red.

terminal B-O bonds are triple bonds and others are single bonds (Figure 4(a)). Note that the distance between the triple bond is farther, the length of the single bond is longer. We confirm that non-uniform distributed delocalized electrons must be existed in the structure. Figure 4(a) gives the π-MOs of 2**I**, which shows that there are six π orbitals in 2**I** (MO = 20, 23, 26, 30, 31, 34). That is, there are 12 electrons delocalized in the whole molecule. In order to get insight into the nature of the bonding in 2**I**, AdNDP analysis was adopted. The AdNDP analysis reveals that 2**I** has four LPs (two on the *sp* hybrid orbital of the terminal O atoms and two on the sp^2 hybrid orbital of the O atoms in the 4-membered ring), ten 2c-2e B-O σ-bonds, four 2c-2e π-bonds on the B-O terminals in two vertical directions, four 3c-2e π-bonds, one 4c-2e π-bond on the 4-membered ring and one 2c-2e π^*-bond (see Figure 4(b)). It is obviously that, as the Lewis structure shows, the terminal B-O bonds are triple bonds and others are single bonds. The five π bonds (ten π-electrons) in *z*-axis direction conjugate with each other on the whole molecule. The two LPs in the p_z orbital of the oxygen atoms in sp^2 hybridization of the 4-membered ring combine into one π orbital and one π^* orbital. The π orbital conjugates with the two empty *p* orbital of the two B atoms. As a result, the energy of the π orbital decreases by the conjugation and the 4-membered ring is stable. The 4-membered ring is aromatic with the NICS value of −9.26 ppm.

3**I** is planar with a planar hexagonal B_3O_3 unit. The B-O bond lengths in 3**I** are 1.21 Å for the three terminal B-O bonds and 1.33 Å–1.38 Å for other B-O bonds. Therefore, the three terminal B-O bonds are considered triple bonds and others are single bonds (Figure 5(a)). Again, the length is longer when the single bond is farther from the triple bond. We suppose there must be non-uniform distributed delocalized electrons in the molecule as the same as found in the GM of $(B_2O_3)_2$. Thirty valence electrons are localized along the ten B-O σ-bonds and 18 electrons are delocalized in the whole molecule according to the MO analysis (nine delocalized π orbitals shown in Figure 5(a)). We applied the AdNDP analysis for the detail information of chemical bonding in 3**I**. AdNDP analysis shows that there are six LPs with three in the terminal O atoms and three in the O atoms of the 6-membered ring, fifteen 2c-2e σ-bonds, six 2c-2e π-bonds, six 3c-2e π-bonds, and three 3c-2e π-bonds (Figure 5(b)), which verifies the supposition to the Lewis structure of the chemical bonding types. The eighteen π-electrons in *z*-axis direction delocalize on the whole molecule which is similar to their delocalized π-MOs and explains the stability of the planar structure. According to Huckel's $4n + 2$ rule for aromaticity, the 6-membered ring is aromatic with six delocalized π electrons which get further support from the NICS value at the ring center (−4.54 ppm).

6**I** is a tetrahedron cage in T_d symmetry. The structure can be regarded as four 6-membered rings occupying the four vertexes of the tetrahedron and another six O atoms at the edges linking the 6-membered ring. The B-O bond lengths are 1.38 Å for the bonding in 6-membered rings and 1.37 Å for the bridging bonding, which means that all the bonds in 6**I** are single bonds. There are 144 valence electrons (3 × 12 + 6 × 18) in total, 72 electrons of which are localized along the 36 B-O σ-bonds. Figure 6(a) plots the 18 π-MOs, which illustrate that there are 36 electrons are delocalized in the whole molecule. The AdNDP bonding patterns are presented in Figure 6(b). The AdNDP analysis shows that there are two

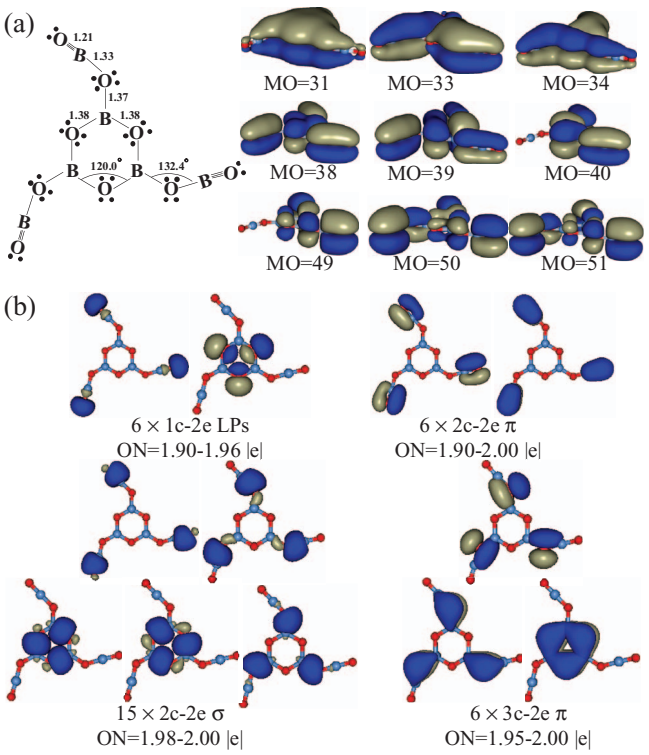

FIG. 5. (a) Lewis representation and π-MOs of 3**I**; (b) AdNDP localized bonding patterns of 3**I**. B-blue, O-red.

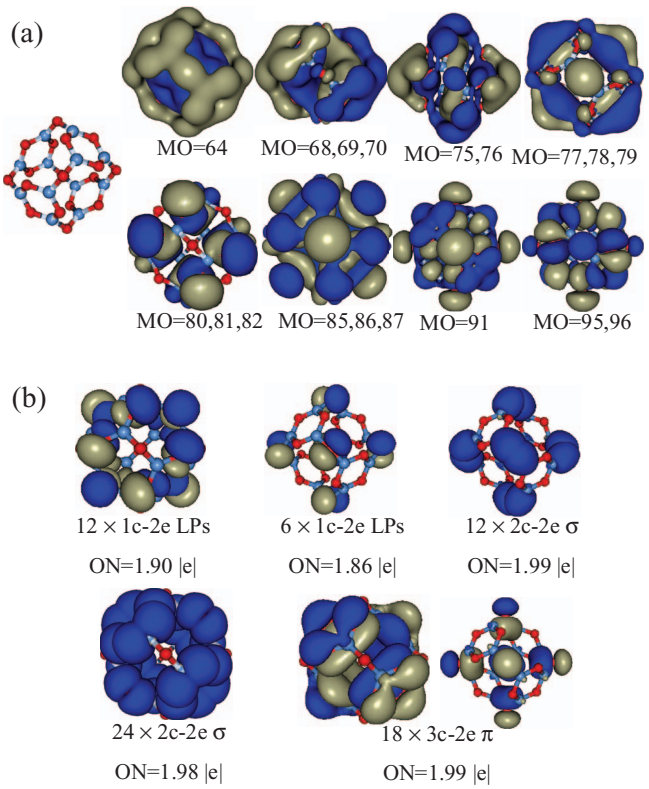

FIG. 6. (a) Structure and π-MOs of 6**I**; (b) AdNDP localized bonding patterns of 6**I**. B-blue, O-red.

kinds of LPs (one on the p_z orbitals of the O atoms in 6-membered rings, and another on the sp^2 hybrid orbitals of the bridging O atoms) with a total number of 18 (ON = 1.86–1.90 |e|), two kinds of σ-bonds (One belongs to 6-membered rings, and another belongs to the edges of the tetrahedron) with a total number of 36 B-O σ-bonds (ON = 1.98–1.99 |e|) and 18 3c-2e B-O-B π-bonds (ON = 1.99 |e|). Verifying the supposition to the Lewis structure, all of the bonds are single σ-bonds. The AdNDP also shows that all of the oxygen atoms are in sp^2 hybridization. The 36 π-electrons are divided into two kinds, one occupies the p orbital of the oxygen in sp^2 hybridization in the 6-membered rings, and another occupies one of the sp^2 hybrid orbitals of the oxygen in the edges of the tetrahedron. The 36 π-electrons delocalized by the entire fullerene, forming the molecular orbitals presented in Figure 6(a). The AdNDP analysis suggests that **6I** is a fullerene, which is consistent with the NICS value of −2.34 ppm in the center of the cage and −2.97 ppm in the center of the 6-membered ring.

D. Discussion

$(B_2O_3)_n$ is sesquioxide the same as $(Al_2O_3)_n$, $(Ga_2O_3)_n$, $(In_2O_3)_n$. There are differences between $(B_2O_3)_n$ and $(Al_2O_3)_n$, $(Ga_2O_3)_n$, $(In_2O_3)_n$ clusters. From $(B_2O_3)_n$ to $(Al_2O_3)_n$, $(Ga_2O_3)_n$ and $(In_2O_3)_n$, the ionicity of bond between two atoms increase, and the covalency decrease gradually. Their cluster structures gradually transform from 2D to 3D. The building-up principle of $(B_2O_3)_n$ is different from that of $(Al_2O_3)_n$, $(Ga_2O_3)_n$, and $(In_2O_3)_n$ clusters. At small size (n = 2 and 3), the GMs of $(Al_2O_3)_n$, $(Ga_2O_3)_n$, and $(In_2O_3)_n$ clusters favor cage and 3D while the GMs of $(B_2O_3)_n$ clusters at that sizes are favor of planes. For n = 4–6, the GMs of $(Al_2O_3)_n$, $(Ga_2O_3)_n$, and $(In_2O_3)_n$ clusters are all 3D, however, the GMs of $(B_2O_3)_n$ clusters are cages. Polarizing nature of boron is very strong, and boron oxides can be regarded as covalent compound. The covalent characteristic of B-O bond results in the structural difference between boron oxides and other IIIA oxides clusters. The particularity of B-O bond makes $(B_2O_3)_n$ clusters have unique structures and properties, which would be potentially applicable in the future. For the larger size of $(B_2O_3)_n$ clusters, cage configuration is supposed to be the GMs.

IV. CONCLUSION

In the present work, the geometric and electronic structures and chemical bonding of a series of small boron oxide clusters $(B_2O_3)_n$ (n = 1–6) are investigated using the method combining the GA with DFT method (TPSSh functional). The low-energy isomers are obtained. The GM structures are planar at n = 1–3, and cage at n = 4–6. We focus on the electronic structure analysis of the GMs of $(B_2O_3)_1$, $(B_2O_3)_2$, $(B_2O_3)_3$, $(B_2O_3)_6$. At n = 1, the V-shaped configuration is more stable than the linear configuration because the center O atom prefers sp^2 hybridization. At n = 2, the delocalized 4c-2e bond explains the stability of the 4-membered ring. There are π electrons delocalized in the whole molecular of planar $(B_2O_3)_3$ and T_d cage $(B_2O_3)_6$. The $(B_2O_3)_n$ clusters prefer 4-membered ring and 6-membered ring because of the stability lead by the delocalized π-bonds in the ring according to the natural bonding analysis given by AdNDP analysis, which also shows that there are many nc-2e bonding patterns in boron oxides. In summary, $(B_2O_3)_n$ clusters favor (quasi-)planar at small size and cage structure at large size. It is due to the electron-deficient p orbital of B element and the electron-rich activity of O element, which result in electrons delocalized in the whole molecule.

ACKNOWLEDGMENTS

This work is supported by the National Natural Science Foundation of China (Grant Nos. 20903001, 21273008), by the 211 Project and by the outstanding youth foundation of Auhui University. The calculations are carried out on the High-Performance Computing Center of Anhui University. We acknowledge Professor Boldyrev for the AdNDP codes.

[1] H. Kato and K. Yamashita, Chem. Phys. Lett. **190**, 361 (1992).
[2] I. Boustani, Phys. Rev. B **55**, 16426 (1997).
[3] V. Bonacic-Koutecky, P. Fantacci, and J. Koutecky, Chem. Rev. **91**, 1035 (1991).
[4] A. K. Ray, I. A. Howard, and K. M. Kanal, Phys. Rev. B **45**, 14247 (1992).
[5] D. Y. Zubarev and A. I. Boldyrev, J. Comput. Chem. **28**, 251 (2007).
[6] L. Rincon, R. Almeida, J. E. Alvarellos, D. Garcia-Aldea, A. Hasmy, and C. Gonzalez, Dalton Trans. **2009**, 3328.
[7] M. L. Drummond, V. Meunier, and B. G. Sumpter, J. Phys. Chem. A **111**, 6539 (2007).
[8] M. Tanimoto, S. Saito, and E. Hirota, J. Chem. Phys. **84**, 1210 (1986).
[9] T. R. Burkholder and L. Andrews, J. Chem. Phys. **95**, 8697 (1991).
[10] A. G. Maki, J. B. Burkholder, A. Sinha, and C. J. Howard, J. Mol. Spectrosc. **130**, 238 (1988).
[11] J. L. Gole, B. Ohllson, and G. Green, Chem. Phys. **273**, 59 (2001).
[12] B. M. Ruscic, L. A. Curtiss, and J. Berkowitz, J. Chem. Phys. **80**, 3962 (1984).
[13] P. G. Wenthold, J. B. Kim, K.-L. Jonas, and W. C. Lineberger, J. Phys. Chem. A **101**, 4472 (1997).
[14] S.-D. Li, H.-J. Zhai, and L.-S. Wang, J. Am. Chem. Soc. **130**, 2573 (2008).
[15] M. Atis, C. Ozdogan, and Z. B. Guvenc, Int. J. Quantum Chem. **107**, 729 (2007).
[16] H. J. Zhai, L. S. Wang, D. Y. Zubarev, and A. I. Boldyrev, J. Phys. Chem. A **110**, 1689 (2006).
[17] S. J. Laplaca, P. A. Roland, and J. J. Wynne, Chem. Phys. Lett. **190**, 163 (1992).
[18] P. A. Roland and J. J. Wynne, J. Chem. Phys. **99**, 8599 (1993).
[19] X. J. Feng and Y. H. Luo, J. Phys. Chem. A **111**, 2420 (2007).
[20] P. A. Hintz, S. A. Ruatta, and S. L. Anderson, J. Chem. Phys. **92**, 292 (1990).
[21] L. Hanley and S. L. Anderson, J. Chem. Phys. **89**, 2848 (1988).
[22] P. A. Hintz, M. B. Sowa, S. A. Ruatta, and S. L. Anderson, J. Chem. Phys. **94**, 6446 (1991).
[23] J. Smolanoff, A. Lapicki, N. Kline, and S. L. Anderson, J. Chem. Phys. **99**, 16276 (1995).
[24] D. Peiris, A. Lapicki, and S. L. Anderson, J. Chem. Phys. **101**, 9935 (1997).
[25] A. Lapicki, D. M. Peiris, J. N. Smolanoff, and S. L. Anderson, J. Chem. Phys. **103**, 226 (1999).
[26] H.-J. Zhai, S.-D. Li, and L.-S. Wang, J. Am. Chem. Soc. **129**, 9254 (2007).
[27] M. T. Nguyen, P. Ruelle, and T.-K. Ha, J. Mol. Struct.: THEOCHEM **104**, 353 (1983).
[28] M. T. Nguyen, Mol. Phys. **58**, 655 (1986).
[29] A. Gupta and J. A. Tossell, Am. Mineral. **68**, 989 (1983).
[30] G. J. Mains, J. Phys. Chem. **95**, 5089 (1991).
[31] J. M. L. Martin, J. P. Francois, and R. Gijbels, Chem. Phys. Lett. **193**, 243 (1992).
[32] M. Brommer and P. Rosmus, J. Chem. Phys. **98**, 7746 (1993).
[33] J. V. Ortiz, J. Chem. Phys. **99**, 6727 (1993).
[34] A. V. Nemukhin and F. Weinhold, J. Chem. Phys. **98**, 1329 (1993).

[35]A. V. Neumukhin and L. V. Serebrennikov, Russ. Chem. Rev. **62**, 527 (1993).
[36]K.-m. Chen, K.-h. Lee, J.-l. Chang, C.-h. Sung, and T.-h. Chung, J. Phys. Chem. **100**, 488 (1996).
[37]A. Papakondylis and A. Mavridis, J. Phys. Chem. A **103**, 9359 (1999).
[38]F. Grein, J. Phys. Chem. A **109**, 9270 (2005).
[39]F. Grein, Chem. Phys. Lett. **418**, 100 (2006).
[40]M. M. Islam, T. Bredow, and C. Minot, Chem. Phys. Lett. **418**, 565 (2006).
[41]C. H. Chin, A. M. Mebel, and D. Y. Hwang, J. Phys. Chem. A **108**, 473 (2004).
[42]W. Z. Yao, J. C. Guo, H. G. Lu, and S. D. Lit, J. Phys. Chem. A **113**, 2561 (2009).
[43]M. T. Nguyen, M. H. Matus, V. T. Ngan, D. J. Grant, and D. A. Dixon, J. Phys. Chem. A **113**, 4895 (2009).
[44]N. Chawla, M. Kerr, and K. K. Chawla, J. Am. Ceram. Soc. **88**, 101 (2005).
[45]Y. Muramatsu, H. Takenaka, T. Oyama, T. Hayashi, M. M. Grush, and R. C. C. Perera, X-Ray Spectrom. **28**, 503 (1999).
[46]H. Effenberger, C. L. Lengauer, and E. Parthe, Monatsch. Chem. **132**, 1515 (2001).
[47]G. E. Gurr, P. W. Montgome, and C. D. Knutson, Acta Crystallogr., Sect. B **26**, 906 (1970).
[48]C. T. Prewitt and R. D. Shannon, Acta Crystallogr., Sect. B **24**, 869 (1968).
[49]X. L. Ding, W. Xue, Y. P. Ma, Z. C. Wang, and S. G. He, J. Chem. Phys. **130**, 014303 (2009).
[50]R. Li and L. Cheng, Comput. Theor. Chem. **996**, 125 (2012).
[51]Y. B. Gu, Q. Di, M. H. Lin, and K. Tan, Comput. Theor. Chem. **981**, 86 (2012).
[52]J. Sun, W. C. Lu, W. Zhang, L. Z. Zhao, Z. S. Li, and C. C. Sun, Inorg. Chem. **47**, 2274 (2008).
[53]S. M. Woodley, Proc. R. Soc. London, Ser. A **467**, 2020 (2011).
[54]L. Ren, L. J. Cheng, Y. Feng, and X. M. Wang, J. Chem. Phys. **137**, 014309 (2012).
[55]Y. Yuan and L. Cheng, Int. J. Quantum Chem. (2012).
[56]L. J. Cheng, J. Chem. Phys. **136**, 104301 (2012).
[57]X. L. Ding, Z. Y. Li, J. H. Meng, Y. X. Zhao, and S. G. He, J. Chem. Phys. **137**, 214311 (2012).
[58]S. Heiles, A. J. Logsdail, R. Schafer, and R. L. Johnston, Nanoscale **4**, 1109 (2012).
[59]C. R. Zhang, H. S. Chen, G. J. Xu, Y. H. Chen, and H. L. Zhang, J. Mol. Struct.: THEOCHEM **805**, 161 (2007).
[60]M. J. Frisch, G. W. Trucks, H. B. Schlegel *et al.*, GAUSSIAN 09, Revision B.01, Gaussian, Inc., Wallingford, CT, 2010.
[61]J. Tao, J. P. Perdew, V. N. Staroverov, and G. E. Scuseria, Phys. Rev. Lett. **91**, 146401 (2003).
[62]L. L. Pan, J. Li, and L. S. Wang, J. Chem. Phys. **129**, 024302 (2008).
[63]C. Adamo and V. Barone, J. Chem. Phys. **110**, 6158 (1999).
[64]Y. Zhao and D. G. Truhlar, J. Chem. Phys. **125**, 194101 (2006).
[65]A. D. Becke, J. Chem. Phys. **98**, 5648 (1993).
[66]W. B. Smith, Magn. Reson. Chem. **37**, 103 (1999).
[67]J. P. Perdew, J. A. Chevary, S. H. Vosko, K. A. Jackson, M. R. Pederson, D. J. Singh, and C. Fiolhais, Phys. Rev. B **48**, 4978 (1993).
[68]G. D. Purvis and R. J. Bartlett, J. Chem. Phys. **76**, 1910 (1982).
[69]A. B. Rahane, M. D. Deshpande, and V. Kumar, J. Phys. Chem. C **115**, 18111 (2011).
[70]P. v. R. Schleyer, C. Maerker, A. Dransfeld, H. Jiao, and N. J. R. v. E. Hommes, J. Am. Chem. Soc. **118**, 6317 (1996).
[71]V. Elser and R. C. Haddon, Nature (London) **325**, 792 (1987).
[72]D. Y. Zubarev and A. I. Boldyrev, Phys. Chem. Chem. Phys. **10**, 5207 (2008).
[73]D. Y. Zubarev and A. I. Boldyrev, J. Org. Chem. **73**, 9251 (2008).
[74]H.-J. Zhai, L.-M. Wang, S.-D. Li, and L.-S. Wang, J. Phys. Chem. A **111**, 1030 (2007).